JOURNAL OF GEOPHYSICAL RESEARCH, VOL. 106, NO. D12, PAGES 12,579–12,588, JUNE 27, 2001

Vertical profiles of cloud condensation nuclei above Wyoming

David J. Delene[1] and Terry Deshler

Department of Atmospheric Science, University of Wyoming, Laramie, Wyoming

Abstract. High-resolution (125 m) profiles of cloud condensation nucleus (CCN) number concentration at 1.0% supersaturation were measured 12 times at Laramie, Wyoming (41°N), and twice at Lauder, New Zealand (45°S), extending from the surface to 200 mbar. The balloon-borne instruments included a condensation nucleus (CN) counter to measure particles with diameter greater than ~10 nm and an optical particle counter to measure particles with diameter >0.3 μm ($D_{0.3}$). Within vertical profiles, variations in CCN concentration were typically positively correlated with changes in CN and $D_{0.3}$ concentrations and often corresponded with changes in relative humidity, typically positively, but occasionally negatively correlated. The aerosol profiles generally show several distinct layers that can be defined by equivalent potential temperature and relative humidity. These layers are used to summarize the 14 vertical profiles by classifying aerosol measurements into five distinct atmospheric layers: surface, lower tropospheric, upper tropospheric, stratospheric and regions of high humidity. Laramie summer and winter profiles show that the mean CCN concentration decreases between the lower and upper tropospheric layers (450 to 130 cm^{-3} in summer, 150 to 65 cm^{-3} in winter). The average summer CCN/CN ratio in Wyoming shows an increase from 0.09 in the lower troposphere to 0.17 in the upper troposphere. The summer CCN concentrations at Lauder, New Zealand, were about twice the summer CCN concentrations measured at Laramie, Wyoming, while the CN and $D_{0.3}$ concentrations were approximately the same.

1. Introduction

The number concentration and activity of cloud condensation nuclei (CCN) influence cloud droplet spectra and hence precipitation processes and cloud albedo [*Hobbs*, 1993; *Jennings*, 1993]. Increases in CCN concentration, resulting from increased SO_2 emissions, have been suggested as possibly offsetting global temperature change expected from increased CO_2 concentrations [*Wigley*, 1989; *Twomey*, 1991]. Aerosols can affect climate directly by scattering and absorbing radiation and indirectly by altering the scattering characteristics of clouds [*Charlson et al.*, 1992]. The direct and indirect climate forcing of aerosols is being considered in global climate models [*Boucher and Anderson*, 1995; *Haywood and Shine*, 1995]; however, our limited understanding in a number of areas has so far precluded a full inclusion of either affect into these models [*Penner et al.*, 1994]. *Chuang et al.* [1997] addressed indirect anthropogenic forcing with a coupled climate/chemistry model to predict changes in the aerosol number spectrum due to anthropogenic sulfate. Using a microphysics model to improve the parameterization of *Ghan et al.* [1993], changes in cloud droplet concentration are related to the aerosol spectrum. *Pan et al.* [1998] investigated indirect forcing of aerosols using the method of *Charlson et al.* [1992] to determine changes in aerosol number concentration due to anthropogenic sulfate and three different parameterizations [*Twomey*, 1977; *Jones et al.*, 1994; *Ghan et al.*, 1993] to relate changes in aerosol number concentration to changes in cloud droplet concentration. They concluded that refining the input parameters might be more important than improving models to minimize uncertainties. Vertical profiles of aerosol size distribution and CCN fraction over continents would provide some of the information required. Here we present high-resolution vertical profiles of CN, CCN, and particles ≥ 0.3 μm over Wyoming, a remote midcontinental North American site.

Several studies have measured continental CCN number concentration near the Earth's surface [*Hudson and Squires*, 1978; *Hudson and Frisbie*, 1991; *Philippin and Betterton*, 1997], and field campaigns have used aircraft to measure continental CCN concentrations aloft [*Hobbs et al.*, 1985; *Hudson and Xie*, 1998]. Figure 1 presents examples of vertical CCN profiles obtained with aircraft using a variety of instruments. The profiles consist of four to six measurements ranging from the surface to a maximum altitude of ~5 km. The profiles show a general decease in CCN concentration with increasing height above the surface but have low vertical resolution. The CCN measurements do not show a systematic decrease in concentration with decreasing supersaturation. Adding to the difficulty in interpreting CCN variations are the inherent difficulties in making good CCN measurements [*Jiusto et al.*, 1981]. Aircraft measurements of CCN have been confined almost exclusively to the lower troposphere. Recent upper tropospheric CCN measurements conducted by *Hudson and Xie* [1998] found constant CCN concentrations with increasing altitude above the lower troposphere.

[1]Now at the Cooperative Institute for Research in Environmental Sciences, University of Colorado/NOAA, Boulder, Colorado.

Paper number 2000JD900800.
0148-0227/01/2000JD900800$09.00

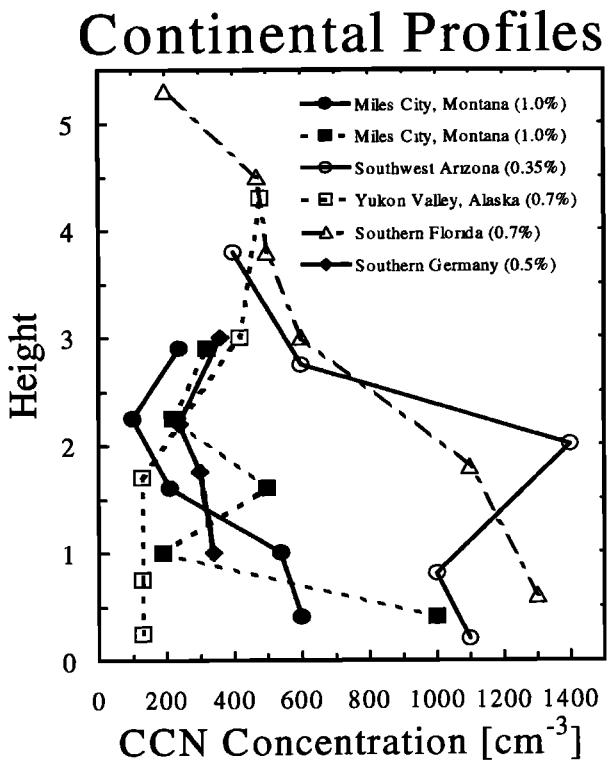

Figure 1. Continental cloud condensation nucleus (CCN) profiles obtained from aircraft measurements. The measurement location and percent supersaturation are given for each profile. The Miles City, Montana, profiles are from *Hobbs et al.* [1985]; the Arizona, Alaska, and southern Florida profiles are from *Hoppel et al.* [1973]; and the southern Germany profile is from *Schafer and Georgii* [1994].

To improve the vertical resolution and altitude range of existing CCN profiles, a balloon-borne CCN counter has been used to obtain 14 CCN profiles extending from the surface to 200 mbar. The CCN counter, operated at a constant supersaturation of 1%, was included on 12 flights at Laramie, Wyoming (41°N), and 2 flights at Lauder, New Zealand (45°S). The 12 flights above Wyoming represent a short climatology of CCN concentration at a midlatitude Northern Hemisphere location, while the 2 flights above New Zealand illustrate the variability of CCN concentrations with location.

2. Instrumentation

Typically, balloon flights start at dawn with clear skies and light winds because of operational constraints. The instrument package consists of three aerosol counters: a CCN counter operated at a constant 1% supersaturation, a condensation nucleus (CN) counter that measures aerosols larger than ~10 nm in diameter, and an optical particle counter (OPC) that measures aerosols with diameter >0.3 μm ($D_{0.3}$). Although the instrument package ascends to a pressure of 10 mbar to measure stratospheric aerosol, the CCN counter is switched off at 200 mbar to avoid overheating resulting from reduced heat transfer at low pressures. It takes ~30 min to obtain an ascent profile to 200 mbar. CCN measurements are obtained every 30 s, providing a vertical resolution of ~125 m. The CN and $D_{0.3}$ measurements are recorded every 10 s, which gives a vertical resolution of ~40 m.

A heater on the common inlet of the aerosol instruments raises the sample air temperature to 40°C during balloon ascent. After passing the heated inlet, the air sample temperature decreases as it flows through 0.8 m of uninsulated stainless steel tubing to each instrument; however, the air entering each instrument remains above the ambient temperature. Thus the humidity is estimated to be <30% at the instrument inlets. Heating the airstream could reduce the size of volatile aerosols by forcing water in the ambient aerosol to evaporate. Changing the ambient aerosol size will affect the measurements to the extent that it reduces the aerosol particles below a threshold size. This will predominantly affect the $D_{0.3}$ measurements. If particle composition were known, it would be possible to theoretically correct the $D_{0.3}$ measurements to replace the water; however, since composition information is not available for these measurements, no corrections are applied. In both the CN and CCN measurements the aerosols are reintroduced to a supersaturated environment prior to measurement. Thus these measurements will only be affected if heating causes the aerosol to shrink below a critical activation size. This was not the case for CN. Several flights with two instruments to compare sampling from a heated and unheated inlet indicate that heating the air sample stream has minimal impact on CN concentrations. Calculations of diffusional loss of aerosol in the heater and sampling inlet indicate <10% particle loss between the surface and 200 mbar for particles >30 nm. Over the same pressure range, diffusional losses for 20-nm particles increase from 10 to 15%, while for 10-nm particles, diffusional losses are about twice as high. Since the true size of the CN particles are not known, no corrections are made for diffusional loss.

The balloon-borne CCN counter uses a static thermal-gradient diffusion chamber to create a supersaturated environment where CCN activate and grow. The CCN concentration is deduced from the amount of laser light scattered by droplets within the diffusion chamber. Measurement uncertainties for CCN concentrations (at ambient pressure) of 50 to 500 cm^{-3} are 36% to 11% owing to counting statistics. The minimum detectable concentration (at ambient pressure) is ~20 cm^{-3}. *Delene et al.* [1998] provided a description of the balloon-borne CCN counter, described calibration at 1% supersaturation on NaCl aerosols, and presented some preliminary CCN profiles. A more complete description of the instrument and its calibration is given by *Delene and Deshler* [2000]. For the measurements presented here, the CCN counter was operated with a plate temperature difference that would create a 1% supersaturation. This plate temperature difference was carefully checked; however, the supersaturation distribution in the chamber has not been measured. Recent measurements of the particle size for 50% activation at 1% supersaturation suggest that the actual supersaturation may be lower than indicated by the plate temperature difference. Work is continuing to further characterize the chamber's supersaturation.

The balloon-borne OPC and CN counter are also University of Wyoming instruments. They are based on the measurement of scattered white light by individual particles passing through the instrument following the design of *Rosen* [1964]. Both counters are continuous flow instruments that count individual particles. The flow rate for each instrument was measured before and after each balloon flight. Typical flow rates are 13 cm^3 s^{-1} for the CN counter and 167 cm^3 s^{-1}

for the OPC. In-flight flow rate measurements are planned for future balloon flights. For the OPC the aerosol size is determined from light intensity measurements at 40° from the forward direction using Mie theory and assuming spherical particles with an index of refraction of 1.45 [*Hofmann and Deshler*, 1991]. The sizing error for particles with indices of refraction between 1.30 and 1.50 is ~10%. For aerosols with diameter >0.3 μm, the uncertainties in concentration are 75% to 2% for concentrations of 0.001 to 1.0 cm^{-3} respectively.

The balloon-borne CN counter is similar to the OPC, except the particles are exposed to a supersaturated environment of ethylene glycol vapor to grow particles to optically detectable sizes [*Rosen and Hofmann*, 1977]. Laboratory tests indicate a counting efficiency of >50% for particles >10 nm with little pressure dependence at pressures between 200 and 75 mbar [*Rozier*, 1993]. To measure tropospheric CN concentrations, the tropospheric air is diluted by a factor of 100 before it enters the CN counter to avoid particle coincidence [*Rosen and Hofmann*, 1977]. In the stratosphere the dilution is removed. Particle coincidence should be considered for undiluted CN concentrations >100 cm^{-3}. The dilution valve is set such that concentrations this high are avoided throughout the flight. For tropospheric (diluted) CN measurements the uncertainties for concentrations of 100 to 1000 cm^{-3} are 8% to 3% owing to counting statistics.

Careful evaluation of each aerosol instrument under tropospheric flight conditions has resulted in some data modifications since the preliminary results of *Delene et al.* [1998]. Connecting the inlet heater to the OPC with 5-mm (inside diameter) stainless steel tubing adds a pressure drop that decreases the laboratory measured flow rate by 5%, resulting in a 5% increase in the aerosol concentration. The added pressure drop is negligible for the low flow rate CN counter. Recent laboratory testing indicates that the actual dilution ratio is greater than used by *Delene et al.* [1998], leading to a correction of the tropospheric CN measurements reported by *Delene et al.* [1998] by a factor of 1.6. Laboratory calibrations of the balloon-borne CCN counter using a higher resolution, greater magnification, lower noise, more light sensitive video camera, and comparisons of the CCN counter to a commercially built CN counter (TSI Incorporated, model 3010 condensation particle counter) resulted in a more accurate absolute calibration of the CCN counter. Thus the CCN concentrations reported here are 18% lower than those reported by *Delene et al.* [1998]. Calibrations with the new video camera have shown that the CCN counter has an accuracy of ~10% at 1% supersaturation [*Delene and Deshler*, 2000].

3. Atmospheric Aerosol Layers

Figure 2 presents measurements of $D_{0.3}$, CCN, CN, temperature, and relative humidity for five balloon ascent profiles in Wyoming and one profile in New Zealand. Seven additional Wyoming profiles and one New Zealand profile are not shown. The aerosol profile shown in Figure 2a is typical of the additional Wyoming profiles not shown here. These profiles show several distinct layers defined by the thermodynamic parameters of equivalent potential temperature and relative humidity. In these profiles the equivalent potential temperature increases in the first 300 m above the surface, is nearly constant or slightly decreases until 5 km above mean sea level, and then increases in the upper troposphere. The relative humidity is nearly constant in the lower troposphere, decreases abruptly at ~5 km, and is relatively constant and <20% in the upper troposphere. The aerosol concentrations are relatively constant from the surface to ~5 km, decrease sharply at ~5 km, and are relatively constant in the upper troposphere. Figures 2b-2f differ from Figure 2a (and the eight profiles not presented) in showing variations in aerosol concentration that correspond to relative humidity changes, in addition to the typical decrease in aerosol concentration between the lower and upper troposphere (at ~5 km for Figure 2a).

The thermodynamic parameters of equivalent potential temperature and relative humidity can be used to group the aerosol measurements into five atmospheric layers: surface, lower troposphere, upper troposphere, stratosphere, and humidity layers. The altitude boundaries of each layer were determined independently for each sounding using a consistent thermodynamic definition. Changes in the boundaries of these layers reflect the influence of many atmospheric processes. Aerosol concentrations above Laramie, Wyoming, are summarized by averaging measurements over the lower and upper tropospheric layers. These layer averages are then compared with two measurements above Lauder, New Zealand. Measurements within the surface, stratospheric, and humidity layers are not extensive enough to provide meaningful averages; however, it is useful to define these layers so that measurements within them can be excluded from the lower and upper tropospheric layers.

Nighttime cooling of air near the Earth's surface produces a temperature inversion resulting in a shallow surface layer. The equivalent potential temperature strongly increases from the bottom to the top of the surface layer; an increase of ~4 K per 200 m is apparent in Figures 2a, 2c, and 2d. The top of the surface layer is located where the equivalent potential temperature starts to increase relatively slowly or is constant with height. The first horizontal solid line above the surface on the right-hand side of the equivalent potential temperature profiles in Figure 2 indicates the top of the surface layer. Figure 2e shows that the aerosol concentration decreases through the surface layer; however, Figure 2a shows no change with height through the surface layer. By examining all of the aerosol profiles, it is evident that concentration changes in the surface layer are most apparent in the smaller sized aerosol. The CN concentration typically decreases sharply while the $D_{0.3}$ concentration decreases very slightly. This may be due to a strong temperature inversion trapping newly produced aerosols. These aerosols could be from the nearby city of Laramie (population 26,000). *Hudson* [1991] points out that even a small coastal town produces a significant increase in CCN concentration. There seems to be a relationship between the strength of the temperature inversion and the degree to which the CN concentration changes from the surface to the bottom of the lower tropospheric layer.

The lower tropospheric layer generally covers the region of convective instability and significant cloud formation in the atmosphere. The lower tropospheric layer extends upward for several kilometers above the surface layer and is capped by the first sharp increase in equivalent potential temperature, an

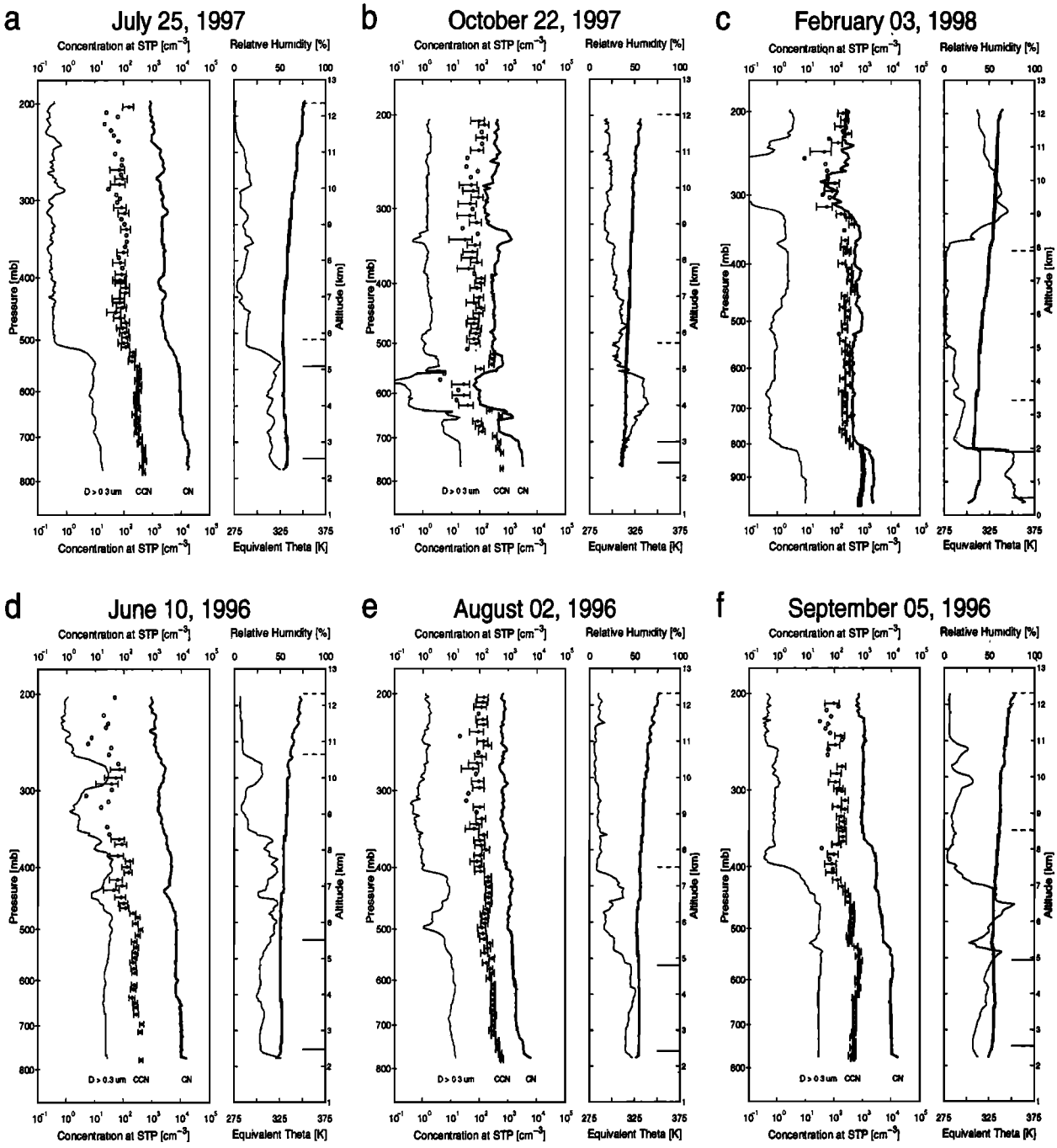

Figure 2. Vertical profiles of particles with diameter > 0.3 μm (D>0.3 μm, thin line), CCN concentration (1% supersaturation, circles), and condensation nucleus (CN) concentration (D>0.01 μm, thick line) at (a) July 25, 1997; (b) October 22, 1997; (c) February 3, 1998; (d) June 10, 1996; (e) August 2, 1996; and (f) September 5, 1996. Open circles represent measurements below the detection limit of the CCN counter. The concentration measured by each aerosol instrument has been corrected to standard temperature and pressure (STP). Equivalent potential temperature (thick line) and relative humidity (thin line) are shown at right. The left axis denotes the measured atmospheric pressure, and the far right axis denotes the altitude above mean sea level. The surface at Laramie, Wyoming, is at ~2.2 km above mean sea level. The horizontal lines on the far right of the equivalent potential temperature plots denote the lower (solid lines) and upper (dashed lines) tropospheric layers. All profiles shown were obtained shortly after sunrise, usually with clear skies and light surface winds. The February 3, 1998, profile is from Lauder, New Zealand. The other five profiles are from Laramie, Wyoming.

increase of ~2 K per 200 m. When a sharp increase in equivalent potential temperature is not present, the first sharp decrease in relative humidity is used to define the top of the lower tropospheric layer. For the examples in Figure 2, relative humidity decreases are used to aid in determining the top of the lower tropospheric layer, the second solid horizontal line above the surface on the right-hand axes in Figure 2. The lower tropospheric layer is similar to a thermodynamically well-mixed layer, but not as narrowly defined. A lower tropospheric layer can always be identified in our profiles. Figure 2a shows an example of the lower tropospheric layer, which runs from near the surface to ~5.1 km. The equivalent potential temperature slowly increases within the layer, followed by a relatively sudden increase above the layer. The relative humidity is nearly constant throughout the layer and decreases sharply above the layer. The lower tropospheric layer has slightly decreasing aerosol concentrations with a sharp decrease above the layer. Aerosol concentrations do not always decrease with height in the lower tropospheric layer as is evident by the slight increases in CCN and CN concentrations observed in the lower tropospheric layer in Figure 2c.

The upper tropospheric layer represents a stable region where equivalent potential temperature increases steadily with height, humidity is low, and there is little variation in humidity. Generally, the upper tropospheric layer extends downward from the top of the sounding (200 mbar), or the stratosphere, until the equivalent potential temperature becomes relatively constant. The upper tropospheric layer is marked in Figure 2 by the two horizontal dashed lines along the right-hand axes and is evident in Figure 2a from ~6 to 12 km. The $D_{0.3}$ and CCN concentrations are constant throughout this layer, while the CN concentration decreases slightly. In the winter, when the tropopause is low, the measurements occasionally extended into the stratosphere. In these cases the top of the upper tropospheric layer is defined by increases in equivalent potential temperature and ozone, which mark the stratosphere. No stratospheric layers are shown in Figure 2. Flights that extend into the stratosphere typically show increases in CCN concentrations in the stratosphere; however, the number of stratospheric CCN layers is too limited to warrant further discussion here. Future measurements are planned to investigate stratospheric CCN.

In addition to the surface, lower, and upper tropospheric layers, which can be identified on all profiles, there are sometimes layers where the relative humidity changes abruptly. Typically, when these humidity layers are present in a balloon ascent profile (Figures 2b-2f), they are not observed during balloon descent. This indicates that the humidity layers have a small horizontal extent (<100 km). CCN concentration changes within humidity layers are usually mirrored by similar changes in $D_{0.3}$ and CN concentrations. Figure 2a presents no humidity layers, while Figures 2b-2f present all the examples of humidity layers found in the data set. For data analysis purposes, measurements near or within humidity layers have been grouped into a layer category separate from the lower and upper tropospheric layers.

Humidity layers can be separated into cases with negative correlation or positive correlation between relative humidity and CCN concentration. Figure 2b at 4 km and Figure 2c at 10 km show negative correlation cases where a relative humidity increase, to a maximum of ~70%, is associated with a decrease in aerosol concentration. Figure 2b at 4 km shows a 2 order of magnitude decrease in $D_{0.3}$ as compared with a 1 order of magnitude decrease in CN. These correlations could be related to cloud processes. A trace amount of precipitation was reported upwind of the flight shown in Figure 2b. The high relative humidity observed in Figure 2c at 10 km suggests that the air was within or near a cirrus cloud. Figure 2d at 6.8 km, Figure 2e at 6.8 km, and Figure 2f at 6.5 km show changes in aerosol concentrations that are positively correlated with relative humidity. The correlation of $D_{0.3}$ with relative humidity is probably not a reflection of particle growth in high humidity layers since the $D_{0.3}$ particles are measured after drying in the inlet heater. Rather, the positive correlation may reflect processing in clouds or humidity layers that may increase gas to particle conversion. *Kleinman and Daum* [1991] observed a correlation between aerosol concentration and water vapor in vertical profiles obtained on 12 aircraft flights, along with some rapid changes in aerosol concentration that corresponded with changes in water vapor. Positive correlation of aerosol and relative humidity may result from an interleaving of air masses with different origins; humidity may also be an important factor in controlling the formation and/or growth of the aerosols [*Salk et al.*, 1986; *Hegg*, 1990; *Perry and Hobbs*, 1994]. Clouds may also be responsible for elevating the CCN concentration within humidity layers [*Saxena and Grovenstein*, 1994; *Radke and Hobbs*, 1991].

4. Summary of Laramie, Wyoming, Aerosol Profiles

The aerosol measurements above Laramie, Wyoming, are grouped into upper and lower tropospheric layers and are also divided into summer (June, July, August, and September; seven balloon flights) and winter (November and January; four balloon flights) categories. The October 22, 1997, balloon flight (Figure 2b) falls between the summer and winter season and is not included in the summary. Figure 3 shows the variability of the lower and upper tropospheric measurements and gives aerosol seasonal averages and standard deviations for the seven summer balloon flights and the four winter balloon flights. The summer averages indicate that between the lower and upper tropospheric layers the $D_{0.3}$ concentration decreases by more than an order of magnitude and the CN and CCN concentrations decrease by factors of 3-6. The winter averages, compared with the summer averages, indicate that between the lower and upper tropospheric layers the $D_{0.3}$ and CCN concentration decrease is not as pronounced, while the CN concentration decrease is similar.

The CCN concentrations presented in Figure 3 are consistent with previous measurements. *Pruppacher and Klett*'s [1997] summary of continental CCN measurements give a range of 600 to 5000 cm^{-3}. The most extensive data to compare with our measurements are those collected by *Hobbs et al.* [1985] over the High Plains of the United States. Frequency distributions of the High Plains CCN measurements indicated two modes: a relatively low CCN concentration mode with mean concentration of 310 cm^{-3} and a higher CCN concentration mode with mean concentration of 2200 cm^{-3}. These concentrations are at 1% supersaturation at ambient pressure, not at standard temperature and pressure (STP). Converting these concentrations to STP would cause a change in concentration of less than a factor of 2 assuming lower tropospheric measurements. *Hobbs et al.* [1985]

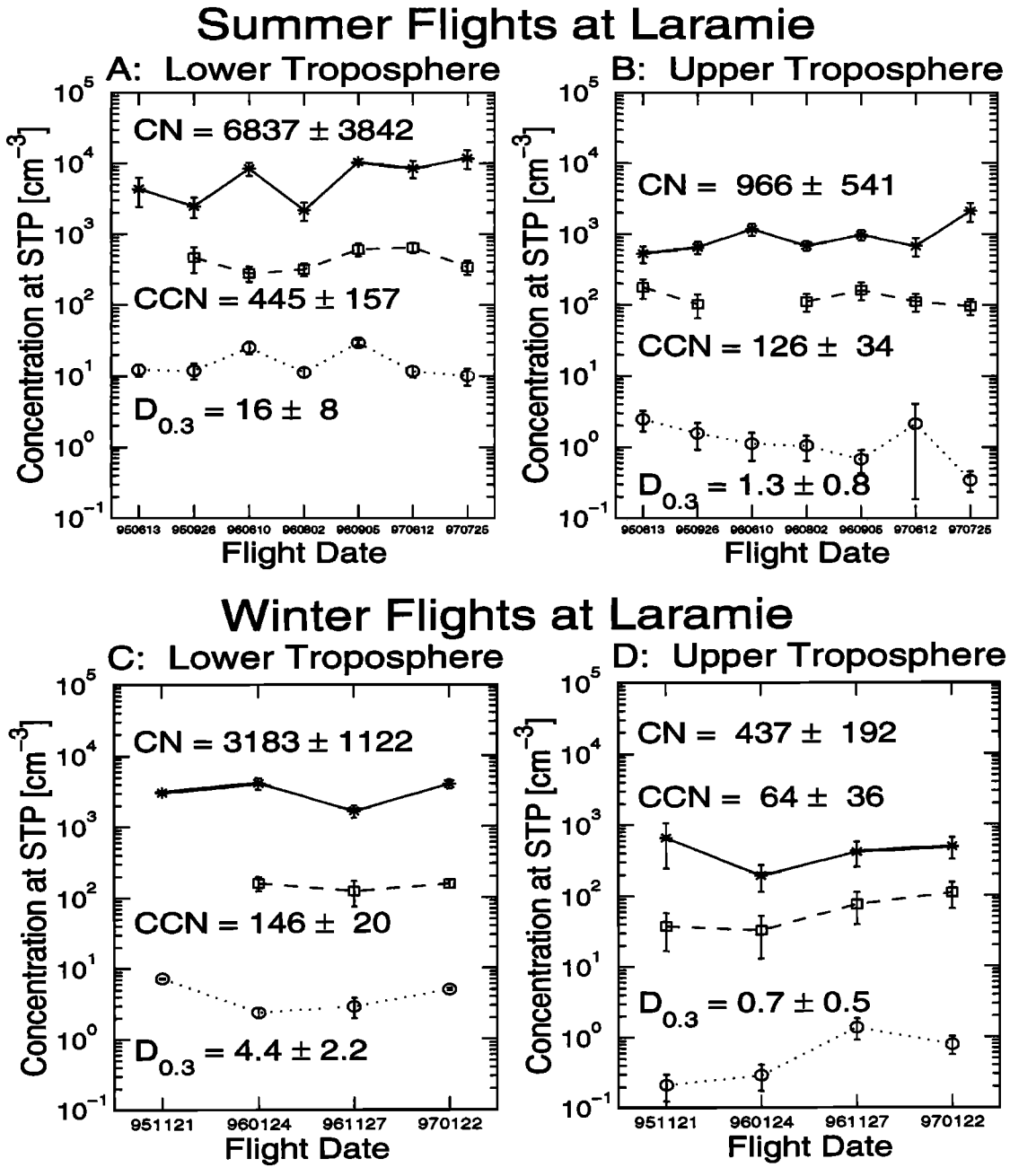

Figure 3. Summer (a) lower and (b) upper troposphere and winter (c) lower and (d) upper troposphere aerosol concentrations from measurements at Laramie, Wyoming, with a balloon-borne optical particle counter (D>0.3 μm, circles), CCN counter (1% supersaturation, squares), and CN counter (D>0.01 μm, asterisks). The error bars represent 1 standard deviation for the measured concentrations within the layer. The aerosol concentrations have been corrected to standard temperature and pressure (STP). The average and standard deviation for the balloon flight data are displayed. Only measurements above the detection limit of the CCN counter are included, so the upper troposphere CCN concentration may be biased to higher concentration, especially for winter measurements. Because of instrument problems, some data are missing.

postulate that the low-concentration mode is the result of a background source of CCN and that the high-concentration mode is due to additional natural and/or anthropogenic sources of CCN. The lower tropospheric CCN concentrations presented in Figure 3 agree with the low "background" CCN concentrations.

The CCN/CN ratio and the $D_{0.3}$/CCN ratio for summer and winter fights at Laramie, Wyoming, are presented in Figure 4. The CCN/CN ratio is larger in the upper troposphere than in the lower troposphere (Figures 4a and 4b) and is relatively consistent between the summer and winter flights. The lower CCN/CN ratio in the lower troposphere is consistent with smaller particles at low altitudes, pointing to a lower atmospheric source of CN. The CCN/CN ratios in the upper troposphere may be low for an aged aerosol, where the median size may be near the activation size for 1% supersaturation; however, the Wyoming CCN/CN ratios are consistent with three studies summarized by *Pruppacher and*

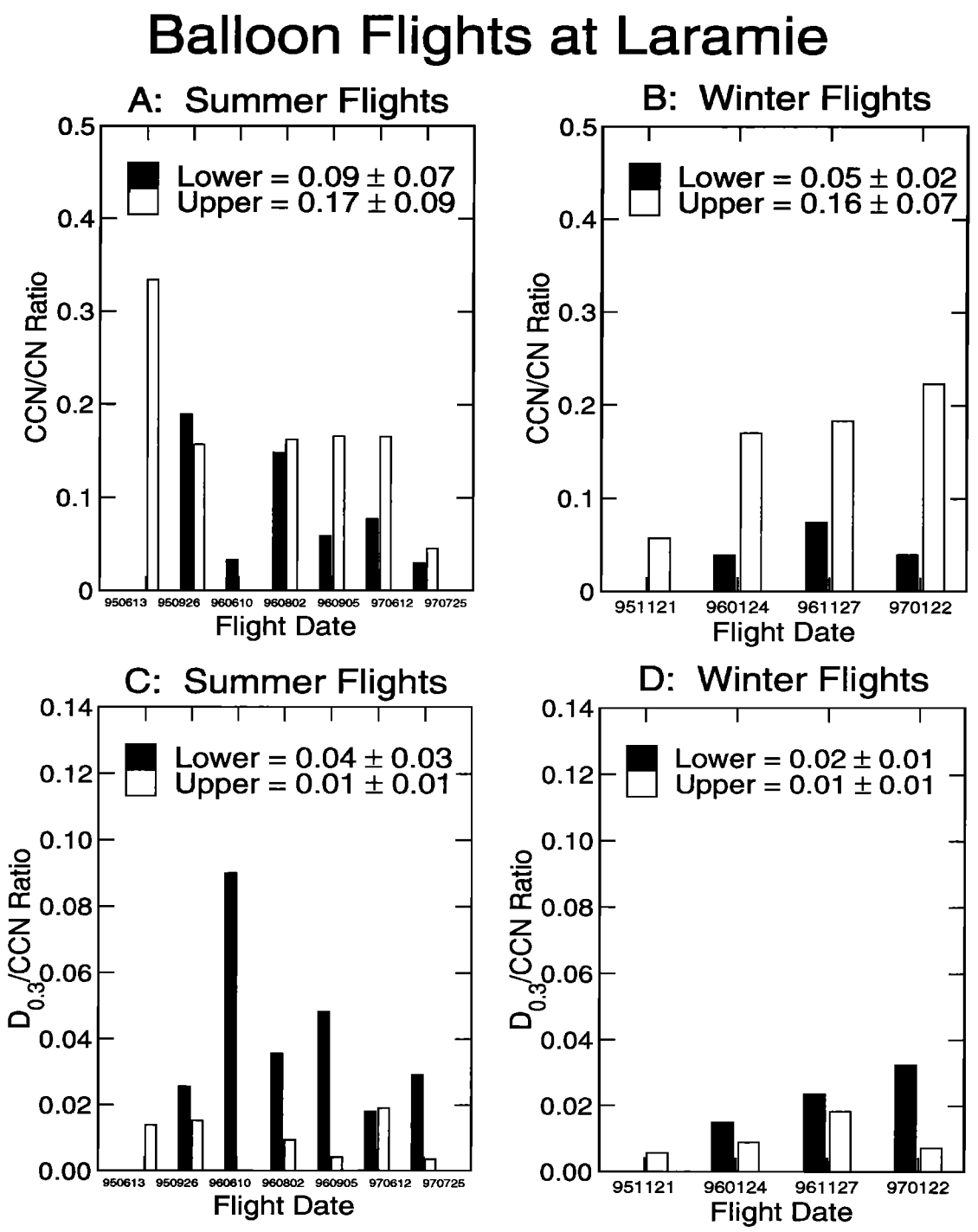

Figure 4. Aerosol ratios, CCN/CN for (a) Summer and (b) winter and $D_{0.3}$/CCN for (c) summer and (d) winter flights, at Laramie, Wyoming. The average and standard deviation for the lower tropospheric and upper tropospheric layers are displayed in the legends. The aerosol ratios are computed by averaging aerosol measurements within a layer and then taking the ratio of the aerosol averages.

Klett [1997], where the continental CCN/CN ratio was from 0.004 to 0.21. In New Zealand the CCN/CN ratio was higher, approaching 1.0 in some cases. The $D_{0.3}$/CCN ratio is larger in the lower troposphere than in the upper troposphere, again pointing to differences in aerosol size distribution and/or solubility. This difference decreases in the winter flights.

Figure 5 presents the percentage vertical change in concentration per kilometer (aerosol vertical gradient) for the lower and upper tropospheric layers. Usually, the CN gradient is the largest. The aerosol gradients for CN, CCN, and $D_{0.3}$ are similar in the upper summer and lower winter troposphere but vary in the lower summer and upper winter troposphere, perhaps reflecting changes in atmospheric mixing summer to winter; however, these observations are not extensive enough to make any generalizations regarding the relationship between aerosol concentrations and meteorological processes.

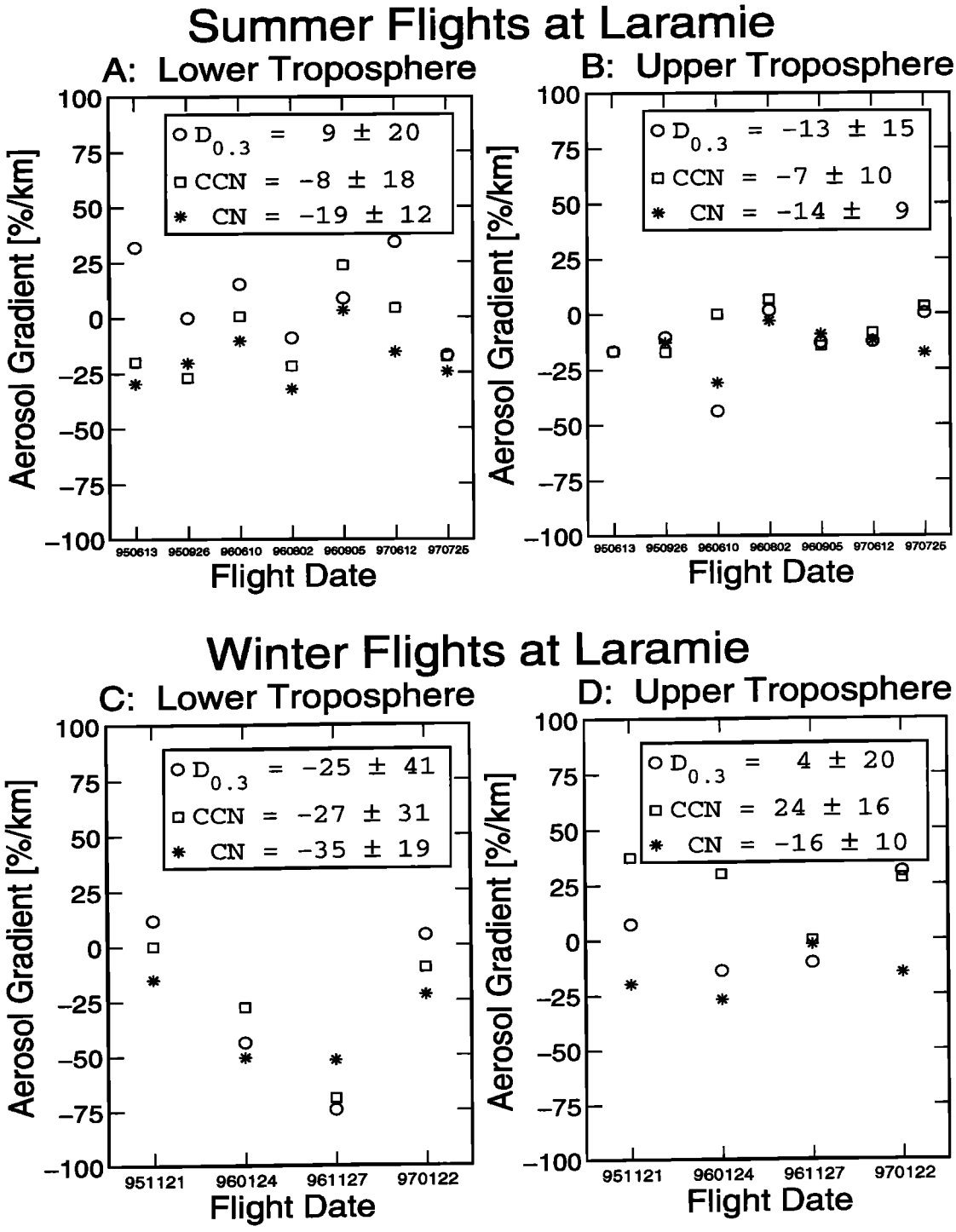

Figure 5. Summer (a) lower and (b) upper troposphere and winter (c) lower and (d) upper troposphere vertical aerosol gradients for $D_{0.3}$ (circles), CCN (squares), and CN (asterisks). Negative gradients indicate a percentage decrease in concentration with increasing height above the surface. The averages and standard deviations of the layer data are displayed in the legends.

5. Comparison Between Wyoming and New Zealand Profiles

As a point of comparison, two balloon flights were conducted at Lauder, New Zealand (45°S), which has a landscape and climate similar to Laramie, Wyoming (41°N). Lauder is ~100 km downwind of the Southern Alps that run along the west coast of the South Island with peak elevations of ~3.0 km. The measurements in Wyoming are obtained ~50-100 km downwind of the Snowy Range with peak elevations of 3.6 km. Although two flights are not enough to form any conclusions, they do provide an interesting contrast to the Wyoming measurements. Table 1 compares the average summer Wyoming measurements with the two New Zealand measurements. The most striking difference is that CCN concentrations are approximately twice as high in New

Table 1. Mean and Standard Deviations of Aerosol Concentrations, Ratios, and Gradients in the Lower and Upper Troposphere for Summer Balloon Flights at Laramie, Wyoming (Seven Flights), and Lauder, New Zealand (Two Flights)

	Laramie, Wyoming		Lauder, New Zealand	
	Lower Troposphere	Upper Troposphere	Lower Troposphere	Upper Troposphere
$D_{0.3}$, cm^{-3}	16 ± 8	1.3 ± 0.8	7.0 ± 1.8	0.9 ± 0.4
CCN, cm^{-3}	445 ± 157	126 ± 34	964 ± 17	246 ± 49
CN, cm^{-3}	6837 ± 3842	966 ± 541	5662 ± 4860	445 ± 206
$D_{0.3}$/CCN	0.041 ± 0.026	0.011 ± 0.006	0.007 ± 0.002	0.004 ± 0.001
CCN/CN	0.09 ± 0.07	0.17 ± 0.09	0.27 ± 0.24	0.59 ± 0.16
$D_{0.3}$ gradient, % km^{-1}	9 ± 20	-13 ± 15	-30 ± 3	18 ± 30
CCN gradient, % km^{-1}	-8 ± 18	-7 ± 10	-3 ± 25	2 ± 0.3
CN gradient, % km^{-1}	-19 ± 12	-14 ± 9	-34 ± 46	-3 ± 8

Definition of the lower and upper troposphere is given in the text and is used consistently for both the Wyoming and New Zealand measurements. $D_{0.3}$ denotes particles with diameter >0.3 μm, CCN is cloud condensation nucleus, and CN is condensation nucleus. The aerosol ratios ($D_{0.3}$/CCN and CCN/CN) are computed by averaging measurements within a layer and then computing the ratio of the aerosol averages. Aerosol gradients ($D_{0.3}$, CCN, and CN) give the percentage change per kilometer in concentration. Negative aerosol gradients indicate a decrease in concentration with increasing height above the surface.

Zealand as in Wyoming, whereas the concentrations of $D_{0.3}$ and CN are similar or lower. This results in New Zealand CCN/CN ratio nearing 1.0 in the upper troposphere on one New Zealand flight. The higher CCN concentrations in New Zealand are not the result of enhanced local pollution since the measured CN and ozone (not shown) concentrations were below the concentrations measured in Wyoming. The larger CCN concentration may be the result of obtaining New Zealand measurements at the height of the seasonal cycle in CCN concentration [*Hobbs et al.*, 1985]; however, none of the Wyoming profiles has CCN concentrations near those obtained in New Zealand. The higher CCN concentration is likely due to differences between the ambient particle size distribution and/or chemical composition in New Zealand compared to Wyoming.

The upper tropospheric CCN measurements above New Zealand agree well with late spring/early summer upper tropospheric measurements made by *Hudson et al.* [1998] of ~200-300 cm^{-3} over the Southern Ocean. This agreement suggests that there is no major change in CCN concentration when upper tropospheric air passes over New Zealand; however, the CCN concentrations reported here are substantially higher in the lower troposphere over New Zealand compared to the marine boundary layer over the Southern Ocean [*Hudson et al.*, 1998]. A similar contrast between marine air and air over New Zealand is observed in the CN concentration. The upper tropospheric New Zealand CN measurements agree with upper tropospheric measurements of ~600 cm^{-3} over the Southern Ocean [*Hudson et al.*, 1998]. In the lower troposphere, however, the New Zealand CN concentrations are substantially larger than measurements of <500 cm^{-3} in the marine boundary layer [*Hudson et al.*, 1998]. The contrast in CN and CCN concentration between marine air and continental air has been observed in previous studies [*Pruppacher and Klett*, 1997]. *Hudson* [1991] observed that surface CN concentrations are much higher 100 km inland, while CCN concentrations are similar.

6. Conclusions

Fourteen, high vertical resolution, midlatitude, continental CCN profiles have been summarized. These CCN profiles were measured with a balloon-borne instrument and have a higher vertical resolution and a greater altitude range than previously available profiles. The CCN profiles were typically obtained near dawn, with clear skies and light surface winds. Concurrent aerosol measurements were also made at smaller (CN) and larger (D>0.3 μm) sizes. The high vertical resolution of the balloon profiles shows that aerosol measurements can be classified into distinct atmospheric layers based on equivalent potential temperature and relative humidity. The profiles reveal that changes in CCN concentration are correlated with changes in the aerosol concentration at other sizes and are associated with humidity changes. A typical profile consists of a relatively constant CCN concentration within the lower tropospheric layer typically from 0.3 to 2.5 km above the surface, a decrease above the lower tropospheric layer, and a relatively constant CCN concentration in the upper troposphere. This typical profile indicates that vertical mixing plays an important role in the distribution of CCN. Differences from this typical profile occur in the presence of humidity layers, which were observed in 5 of the 14 CCN profiles. Concentration changes associated with humidity layers are evident in the three different aerosol size measurements, CN, CCN, and $D_{0.3}$.

The average summer lower and upper tropospheric CCN concentration at Laramie, Wyoming (445 ± 157 and 126 ± 34, respectively), shows little variability between flights conducted under similar meteorological conditions. The average summer CCN/CN ratio in Wyoming shows an increase from 0.09 in the lower troposphere to 0.17 in the upper troposphere. The CCN/CN ratio increases between the lower and upper troposphere, indicating differences in the size distribution and/or composition of the aerosol. Aerosol gradients within the lower and upper tropospheric layers show relatively small percentage changes within the layers and indicate that the smaller-sized aerosol have the largest percentage decrease with increasing height above the surface. The decrease in CCN concentration between the lower and upper troposphere and the typical negative gradient in CCN concentration within the lower troposphere suggest a CCN source near the surface. Two measurements of CCN profiles above New Zealand indicate concentrations that are approximately twice as high, in both the lower and upper troposphere, as CCN concentrations in Wyoming. Although

suggestive of a difference in CCN concentration between these two sites, further measurements in the Southern Hemisphere are required to establish this difference.

Acknowledgments. Lyle Womack and Jason Gonzales provided engineering support in conducting balloon flights. Jefferson Snider, Perry Wechsler, and Gabor Vali provided valuable support, suggestions, and comments. Assistance with the balloon flights by the personnel of NIWA at Lauder, in particular, Brian McNamara, is gratefully acknowledged. This research was supported by grants from the National Aeronautics and Space Administration and the National Science Foundation.

References

Boucher, O., and T. L. Anderson, General circulation model assessment of the sensitivity of direct climate forcing by anthropogenic sulfate aerosols to aerosol size and chemistry, *J. Geophys. Res.*, *100*, 26,117-26,134, 1995.

Charlson, R. J., S. E. Schwartz, J. M. Hales, R. D. Cess, J. A. Coakley Jr., J. E. Hansen, and D. J. Hofmann, Climate forcing by anthropogenic aerosols, *Science*, *255*, 423-430, 1992.

Chuang, C. C., J. E. Penner, K. E. Taylor, A. S. Grossman, and J. J. Walton, An assessment of the radiative effects of anthropogenic sulfate, *J. Geophys. Res.*, *102*, 3761-3778, 1997.

Delene, D. J., and T. Deshler, Calibration of a photometric cloud condensation nucleus counter designed for deployment on a balloon package, *J. Atmos. Oceanic Technol.*, *17*, 459-467, 2000.

Delene, D. J., T. Deshler, P. Wechsler, and G. A. Vali, A balloon-borne cloud condensation nuclei counter, *J. Geophys. Res.*, *103*, 8927-8934, 1998.

Ghan, S. J., C. C. Chuang, and J. E. Penner, A parameterization of cloud droplet nucleation, Single aerosol type, *Atmos. Res.*, *30*, 197-221, 1993.

Haywood, J. M., and K. P. Shine, The effect of anthropogenic sulfate and soot aerosol on the clear sky planetary radiation budget, *Geophys. Res. Lett.*, *22*, 603-606, 1995.

Hegg, D. A., Heterogeneous production of cloud condensation nuclei in the marine atmosphere, *Geophys. Res. Lett.*, *17*, 2165-2168, 1990.

Hobbs, P. V., *Aerosol--Cloud--Climate Interactions*, pp. 33-73, Academic, San Diego, Calif., 1993.

Hobbs, P. V., D. A. Bowdle, and L. F. Radke, Particles in the lower troposphere over the High Plains of the United States, II, Cloud condensation nuclei, *J. Clim. Appl. Meteorol.*, *24*, 1358-1369, 1985.

Hofmann, D. J., and T. Deshler, Stratospheric cloud observations during formation of the Antarctic ozone hole in 1989, *J. Geophys. Res.*, *96*, 2897-2912, 1991.

Hoppel, W. A., J. E. Dinger, and R. E. Ruskin, Vertical Profiles of CCN at Various Geographical Locations, *J. Geophys. Res.*, *30*, 1410-1420, 1973.

Hudson, J. G., Observations of anthropogenic cloud condensation nuclei, *Atmos. Environ., Part A*, *25A*, 2449-2455, 1991.

Hudson, J. G., and P. R. Frisbie, Surface cloud condensation nuclei and condensation nuclei measurements at Reno, Nevada, *Atmos. Environ., Part A*, *25A*, 2285-2299, 1991.

Hudson, J. G., and P. Squires, Continental surface measurements of CCN flux, *J. Atmos. Sci.*, *35*, 1289-1295, 1978.

Hudson, J. G., and Y. Xie, Cloud condensation nuclei measurements in the high troposphere and in jet aircraft exhaust., *Geophys, Res. Lett.*, *25*, 1395-1398, 1998.

Hudson, J.G., Y. Xie, and S. S. Yum, Vertical distributions of cloud condensation nuclei spectra over the summertime Southern Ocean, *J. Geophys. Res.*, *103*, 16,609-16,624, 1998.

Jennings, S G., *Aerosol Effects on Climate*, pp. 275-297, Univ. of Ariz. Press, Tucson, 1993.

Jiusto, J. E., R. E. Ruskin, and A. Gagin, CCN comparisons of static diffusion chambers, *J. Rech. Atmos.*, *15*, 291-302, 1981.

Jones, A., D. L. Roberts, and A. Slingo, A climate model study of indirect radiative forcing by anthropogenic sulphate aerosols, *Nature*, *370*, 450-453, 1994.

Kleinman, L. I., and P. H. Daum, Vertical distribution of aerosol particles, water vapor, and insoluble trace gases in convectively mixed air, *J. Geophys. Res.*, *96*, 991-1005, 1991.

Pan, W., M. A. Tatang, G. J. McRae, and R. G. Prinn, Uncertainty analysis of indirect radiative forcing by anthropogenic sulfate aerosols, *J. Geophys. Res.*, *103*, 3815-3823, 1998.

Penner, J. E., R. J. Charlson, J. M. Hales, N. S. Laulainen, R. Leifer, T. Novakov, J. Ogren, L. F. Radke, S. E. Schwartz, and L. Travis, Quantifying and minimizing uncertainty of climate forcing by anthropogenic aerosols, *Bull. Am. Meteorol. Soc.*, *75*, 375-400, 1994.

Perry, K. D., and P. V. Hobbs, Further evidence for particle nucleation in clear air adjacent to marine cumulus clouds, *J. Geophys. Res.*, *99*, 22,803-22,818, 1994.

Philippin, S., and E. A. Betterton, Cloud condensation nuclei concentrations in Southern Arizona: Instrumentation and early observations, *Atmos. Res.*, *43*, 263-275, 1997.

Pruppacher, H. R., and J. D. Klett, *Microphysics of Clouds and Precipitation*, pp. 287-289, Kluwer Acad. Norwell, Mass., 1997.

Radke, L. F., and P. V. Hobbs, Humidity and particle fields around some small cumulus clouds, *J. Atmos. Sci.*, *48*, 1190-1193, 1991.

Rosen, J. M., The vertical distribution of dust to 30 km, *J. Geophys. Res.*, *69*, 4673-4676, 1964.

Rosen, J. M., and D. J. Hofmann, Balloonborne measurements of condensation nuclei, *J. Appl. Meteorol.*, *16*, 56-62, 1977.

Rozier, W. R., Analysis of a balloonborne, continuous flow condensation nuclei growth chamber, M. S. thesis, 85 pp., Univ. of Wyo., Laramie, December 1993.

Salk (Suck) S. H., R. E. Thurman, and C. H. Kim, Growth of ultrafine particles by brownian coagulation, *Atmos. Environ.*, *20*, 773-777, 1986.

Saxena, V. K., and J. D. Grovenstein, The role of clouds in the enhancement of cloud condensation nuclei concentrations, *Atmos. Res.*, *31*, 71-89, 1994.

Schafer, B., and H. W. Georgii, Airborne measurements of condensation nuclei and cloud condensation nuclei above the Alpine Foothills, *Contrib. Atmos. Phys.*, *67*, 225-340, 1994.

Twomey, S., *Atmospheric Aerosols*, Elsevier, New York, 1977.

Twomey, S., Aerosols, clouds and radiation, *Atmos. Environ., Part A*, *25A*, 2435-2442, 1991.

Wigley, T. M. L., Possible climate change due to SO_2-derived cloud condensation nuclei, *Nature*, *339*, 365-367, 1989.

D. Delene Scientific Computing Research Associate, University of North Dakota, John D. Odegard School of Aerospace Sciences, University Avenue & Tulana Drive, Grand Forks, ND 58202-9007. (delene@umac.org)

T. Deshler, Departemnt of Atmospheric Science, University of Wyoming, Laramie, WY 82071.

(Received February 7, 2000; revised October 4, 2000; accepted October 4, 2000.)